Quasi-Static Operation of 2-Axis-Tilt Microscanners with AlN Piezoelectric Quad-Actuators

Dooyoung Hah
Department of Electrical and Electronics Engineering
Abdullah Gül University
Kayseri, Turkey
dooyoung.hah@agu.edu.tr

2021 Symposium on Design, Test, Integration & Packaging of MEMS and MOEMS (DTIP) | 978-1-6654-0230-9/21/$31.00 ©2021 IEEE | DOI: 10.1109/DTIP54218.2021.9568679

***Abstract*—Aluminum nitride (AlN) started to draw attentions as a material for piezoelectric actuation owing to its CMOS process compatibility and safeness for biomedical applications. Due to its relatively low piezoelectric coefficients, AlN-based piezoelectric actuators have been mostly operated in resonance modes, especially in optical scanning. This paper presents a novel design of a 2-axis-tilt microscanner with AlN piezoelectric quad-actuators and meander-shaped hinges for reasonable quasi-static operation. Through finite-element-method simulation, it is shown that the proposed device can have about 9 degree of optical scan angle in two dimensions with the voltage amplitude of 50 V. Lissajous scanning operation of the device is demonstrated as well via simulation.**

Keywords— Microscanner, piezoelectric actuator, aluminum nitride

I. Introduction

Piezoelectric actuation has several merits for optical microscanning, such as low power consumption and linear voltage-angle relationships. Lead zirconate titanate (PZT) has been most widely employed for its high piezoelectric coefficients ($|d_{31}| > 100$ pC/N) [1-3]. Recently, aluminum nitride (AlN) started to draw attentions as an alternative material because its fabrication processes are compatible with those of CMOS. Availability of a foundry service employing AlN as the piezoelectric material, e.g. MEMSCAP's PiezoMUMPs, is another advantage. Most importantly, AlN is a safe material, which is especially crucial in biomedical applications. Lead and lead compounds have been being faded out globally due to the effects to the human health, exemplified by the Restriction of Hazardous Substances Directive (RoHS).

The main drawback of AlN for actuator applications is its relatively low piezoelectric coefficients. The magnitude of AlN's d_{31} is just a few pC/N, orders of magnitude smaller than that of PZT [4-6]. Therefore, AlN-based optical microscanners reported so far have been only operated in resonance modes [7-8]. Although mechanical amplification by resonance is attractive on one hand, process-variation-induced shift and long-term drift of resonant frequencies jeopardize reliable operation in the long term. For this reason, this paper presents quasi-static operation of AlN-based microscanners by incorporating a novel quad-actuator and a meander-shaped-hinge design.

This work was partially supported by Research Fund of the Abdullah Gül University (Project Number: FOA-2016-49).

II. Device Structure and Operation Principle

Fig. 1 illustrates the structure of the proposed micro-scanner. It has four actuators connected to a mirror through four hinges. When a voltage is applied to it, an actuator is deflected either upwards or downwards depending on the polarity of the voltage. This vertical movement is translated into a rotation of the mirror through deformations of the hinges. In order to make this translation more efficient, hinges are meander shaped so that they not only bend along *x*-axis but also twist about it.

Fig. 2 shows the finite-element-method (FEM) simulation results (COMSOL Multiphysics®) that demonstrate rotation of the mirror by the actuation of the quad-actuators. By lifting actuators 1 and 3, and lowering actuators 2 and 4, clockwise rotation about *x*-axis is achieved (Fig. 2, top). By lifting actuators 1 and 2 while lowering actuators 3 and 4 (Fig. 2, middle), counterclockwise rotation about *y*-axis is obtained. By lifting actuator 1 and lowering actuator 4 (Fig. 2, bottom), rotation in diagonal direction is realized.

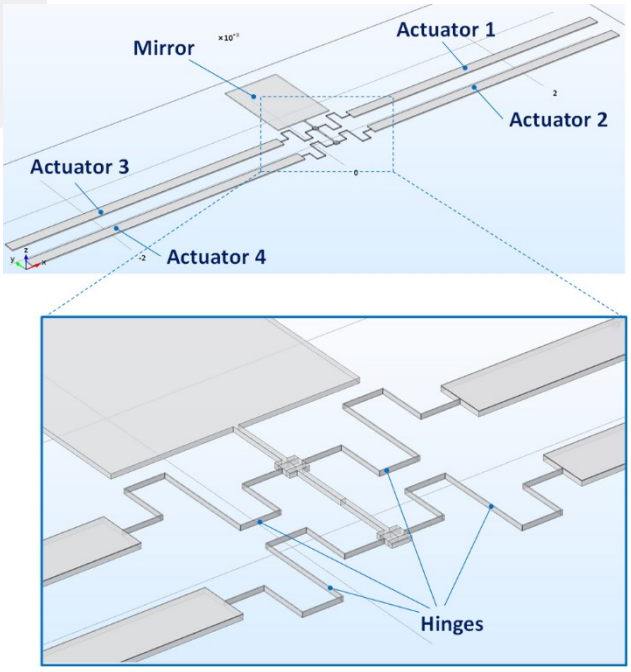

Fig. 1. Proposed microscanner with quad-actuators and meander-shaped-hinges. Layer structure (from bottom): Si/AlN/Al.

978-1-6654-0230-9/21/$31.00 ©2021 IEEE

TABLE I. DEVICE GEOMETRIES AND MATERIAL PROPERTIES

Description	*Symbol*	*Value*
Mirror length	L_M	500 µm
Mirror width	W_M	700 µm
Actuator length	L_A	2500 µm
Actuator width	W_A	100 µm
Hinge width	W_h	2 µm
Silicon device layer thickness	T_{Si}	10 µm
AlN layer thickness	T_{AlN}	500 nm
Al electrode layer thickness	T_{Al}	1 µm
Silicon Young's modululs	E_{Si}	170 GPa
Aluminum Young's modulus	E_{Al}	70 GPa
AlN piezoelectric constant	d_{31}	-1.73 pC/N
AlN compliance	s^E_{11}	0.0029 $(GPa)^{-1}$

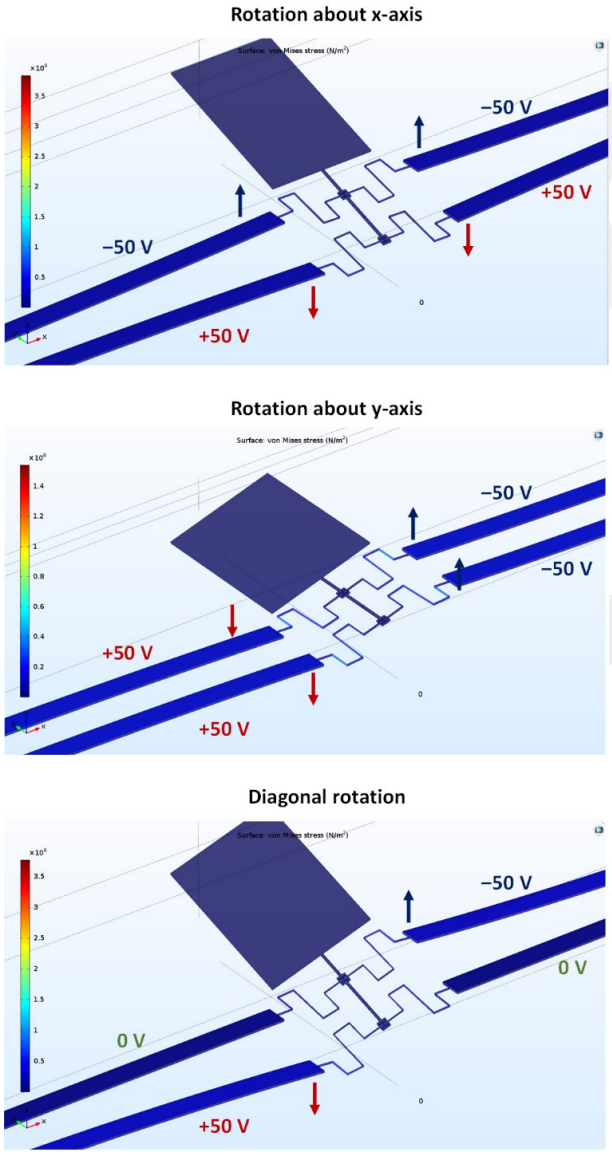

Fig. 2. *FEM simulation results. Applied dc voltages are written next to each of the actuators. Rotation about (top) x-axis, (middle) y-axis, (bottom) x- and y-axis.*

III. SIMULATION RESULTS

The performances of the proposed microscanner was studied numerically by using COMSOL Multiphysics®. The layer structure (Si/AlN/Al) and the individual layer thickness (as written in Table I) follow those of PiezoMUMPs process. Table I also presents the device geometries and the material properties used in the study. The mirror dimensions were determined, based on the system setup of the specific biomedical imaging application. The hinge width was decided as the minimum allowed linewidth in the PiezoMUMPs process. In the PiezoMUMPs process, there is a very thin (20 nm) layer of chromium between AlN and aluminum, which was ignored in the simulation for its thinness.

A. Hinge Optimization

One of the most important design parameters is the dimensions of the meander hinges. A shorter hinge section limits its deformation while a longer hinge section results in inefficient conversion from deformation to rotation. Therefore, an optimum length combination, i.e. the longitudinal section length (L_{hV}, x-axis) and the lateral section length (L_{hH}, y-axis), was sought with the goal of maximizing θ_{min}. θ_{min} is defined as the lower value between the rotation angles in two axes, θ_x and θ_y for a given hinge combination. This strategy was set up, aiming maximum utilization of an image plane, which can be obtained through a symmetrical optical probe in biomedical imaging application.

Fig. 3 shows the calculated rotation angles in two axes

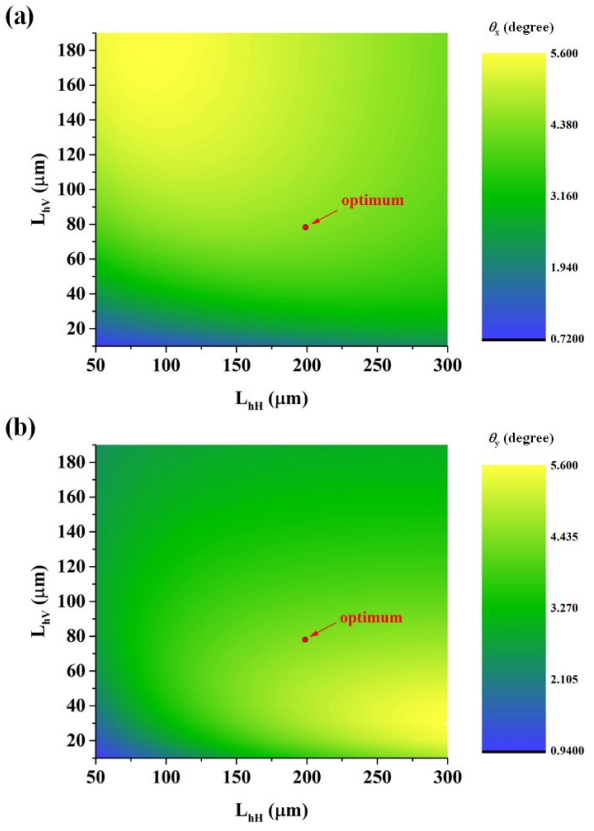

Fig. 3. Simulation results of mechanical rotation angles about (a) x-axis (θ_x) and (b) y-axis (θ_y) for various hinge dimensions, L_{hV} (longitudinal section) and L_{hH} (lateral section). Applied voltage to each actuator is either 50 V or -50 V according to schemes illustrated in Fig. 2. Optimum hinge dimensions are indicated in the maps.

for different hinge combinations. As can be seen from Fig. 3, shorter L_{hH} and longer L_{hV} are advantageous for higher θ_x while longer L_{hH} and shorter L_{hV} are desirable for higher θ_y. This implies that there is an optimum set of hinge lengths for higher θ_{min}. As indicated in Fig. 3, for the given actuator dimensions, optimum lengths for the hinge sections are found as 78 μm (L_{hV}) and 199 μm (L_{hH}), which results in an optical scan angle of about 18 degree in two dimensions.

It is important to make sure that stress experienced by the structure during operation is within the limit of the material. Fig. 4 shows the calculated von Mises stress for various conditions. Diagonal rotation results in the highest stress in the amount of 290 MPa while in the case of rotation about a single axis (*x*- or *y*-), it is 145 MPa. This stress level is significantly lower than the bending strength (7-11 GPa) of micrometer-level single crystalline silicon structures, reported in [9].

B. 2-D Scanning

FEM simulation was continued to test the two-dimensional (2-D) rotation of the proposed device with the optimum hinge dimensions, found in the previous section. Fig. 5 shows the voltage maps for the quad-actuator to realize 2-D scanning. As can be expected intuitively, there are symmetries among voltage maps of the four actuators. With the proposed scanner configuration, the maximum continuous areal scan angle (in one axis) is a half of the linear scan angle, which results in the optical scan angles of about 9 degree in 2-D.

Next, the proposed device was characterized in frequency domain as well as in time domain via FEM simulation. The resonant frequencies were found as 464 Hz (rotation about *x*-axis) and 2030 Hz (rotation about *y*-axis). Two scanning modes were tested: a raster-like mode and a Lissajous mode [10], and it was found out that the latter can provide denser scanning coverage for a bit lower frame rate.

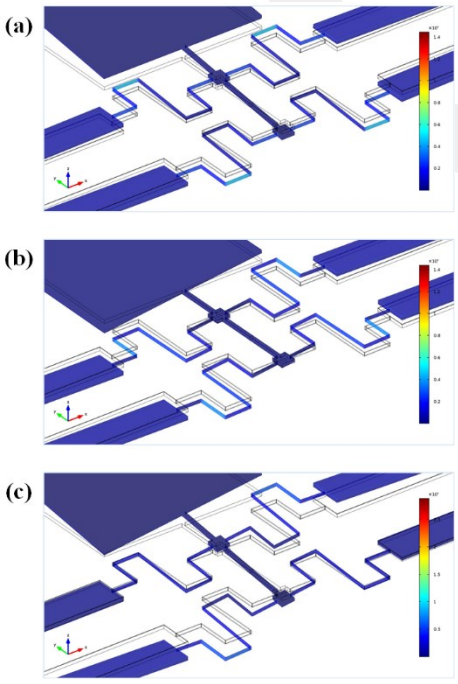

Fig. 4. Calculated von Mises stress. Voltages applied to actuators 1, 2, 3, and 4: (a) –25 V, 25 V, –25 V, 25 V, (b) –25 V, –25 V, 25 V, 25 V, and (c) –50 V, 0 V, 0 V, 50 V.

For both modes, the voltage applications are as follows.

$$v_1(t) = V_0(-\sin 2\pi f_1 t - \sin 2\pi f_2 t) \quad (1)$$

$$v_2(t) = V_0(\sin 2\pi f_1 t - \sin 2\pi f_2 t) \quad (2)$$

$$v_3(t) = V_0(-\sin 2\pi f_1 t + \sin 2\pi f_2 t) \quad (3)$$

$$v_4(t) = V_0(\sin 2\pi f_1 t + \sin 2\pi f_2 t) \quad (4)$$

v_i is the voltage for the actuator *i*. V_0 is the voltage amplitude. f_1 and f_2 are operation frequencies. *t* is time. Fig. 6 shows the Lissajous scan pattern obtained via FEM when V_0, f_1, and f_2 are 50 V, 111 Hz, and 100 Hz, respectively.

IV. Conclusion

A 2-axis-tilt microscanner configuration was proposed, which employs an AlN piezoelectric quad-actuator and meander-shaped hinges, for quasi-static operation in biomedical imaging applications. Finite element analysis was

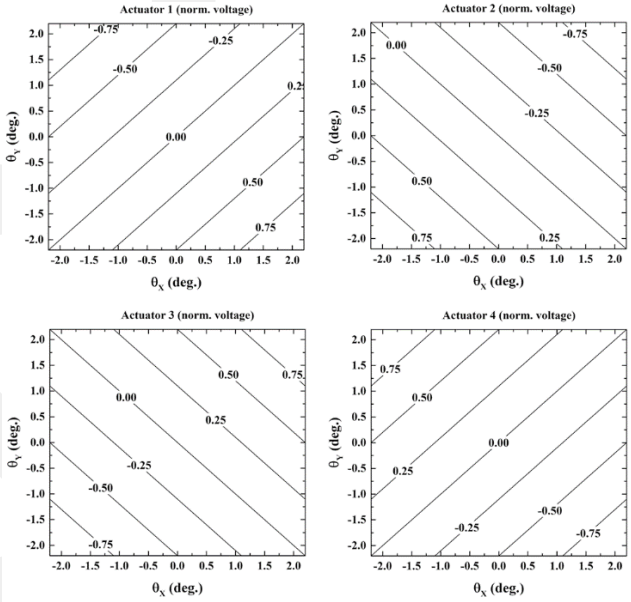

Fig. 5. Voltage (normalized) contour maps to achieve specific rotation angles in 2-D by the proposed microscanner with optimized hinges. Clockwise from top-left: actuator 1, actuator 2, actuator 4, and actuator 3.

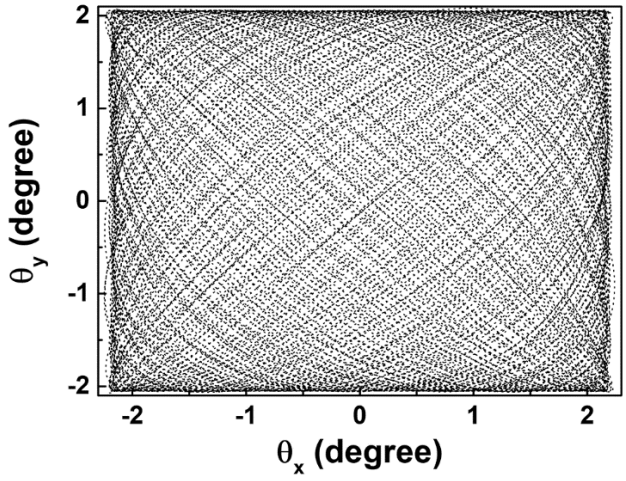

Fig. 6. Lissajous scan pattern of the proposed microscanner, simulated by using FEM. V_0 = 50 V, f_1 = 111 Hz, and f_2 = 100 Hz.

used to demonstrate the proof of concept, to study the device characteristics, and to design the devices in a detailed manner. Through the study, the optimum design was identified. The study showed that the proposed device can have an optical scan angle of 9 degree in two dimensions. Lissajous scanning by the proposed microscanner was demonstrated as well via simulation. Further works include the fabrication of the microscanner by using PiezoMUMPs and characterization of the fabricated devices.

REFERENCES

[1] Dubois MA, Muralt P, Taylor DV, Hiboux S, "Which PZT thin films for piezoelectric microactuator applications?" Int. Ferroelec., vol. 22, pp. 535-543, 1998.

[2] Piekarski B, Dubey M, Zakar E, Polcawich R, Devoe D, and Wickenden D, "Sol-gel PZT for MEMS applications," Int. Ferroelec., vol. 42, pp. 25-37, 2002.

[3] Polcawich RG, et al., "Design and fabrication of a lead zirconate titanate (PZT) thin film acoustic sensor," Int. Ferroelec., vol. 54, pp. 595-606, 2003.

[4] Tsubouchi K and Mikoshiba N, "Zero-temperature-coefficient SAW devices on AlN epitaxial films," IEEE Trans. Sonics Ultrason., vol. SU-32, pp. 634-644, 1985.

[5] Trolier-McKinstry S and Muralt P, "Thin film piezoelectrics for MEMS," J. Electroceramics, vol. 12, pp. 7-17, 2004.

[6] Zuo C, Sinha N, Van der Spiegel J, and Piazza G, "Multi-frequency pierce oscillators based on piezoelectric AlN contour-mode MEMS resonators," In 2008 IEEE Int. Freq. Control Symp., pp. 402-407, 2008.

[7] Shao J, Li Q, Feng C, Li W, and Yu H, "AlN based piezoelectric micromirror," Opt. Lett., vol. 43, pp. 987-990, 2018.

[8] Meinel K, et al., "Piezoelectric scanning micromirror with large scan angle based on thin film aluminum nitride," in Proceedings of the Transducers 2019, pp. 1518-1521, 2019.

[9] Namazu T, Isono Y, and Tanaka T, "Evaluation of size effect on mechanical properties of single crystal silicon by nanoscale bending test using AFM," J. Microelectromech. Syst., vol. 9, pp. 450-459, 2000.

[10] Wang J, Zhang G, and You Z, "Design rules for dense and rapid Lissajous scanning," Microsyst. Nanoeng., vol. 6, 101, 2020.